



Cite this: *Green Chem.*, 2021, **23**, 8453

Received 11th August 2021,  
Accepted 13th October 2021

DOI: 10.1039/d1gc02889h

rsc.li/greenchem

Core-shell  $\text{SiO}_2@\text{Au@TiO}_2$  materials have shown excellent catalytic performances in the base-free oxidation of furfural (FF) to furoic acid (FA). The enhanced catalytic behaviour with respect to that observed over supported  $\text{SiO}_2@\text{TiO}_2@\text{Au}$  catalysts suggests a key role of the  $\text{TiO}_2$  shell, which could prevent Au deactivation by irreversible FA adsorption, improve metal–oxide interaction and presumably, give rise to the formation of new active sites located at the perimeter of the  $\text{Au–TiO}_2$  interface.

With anthropogenic climate change and depletion of fossil fuels being major concerns in our days, a shift in the energy paradigm towards a “green” future has become imperative.<sup>1-3</sup> In this context, the use of lignocellulosic biomass as a feedstock to produce biofuels, energy, and renewable chemicals appears as a promising alternative for reducing greenhouse gases (GHGs) emissions and for mitigating climate change.<sup>4-7</sup>

Among the lignocellulosic biomass derivatives, furfural (FF) belongs to the top 10 platform molecules, which can be further valorised into various key chemicals.<sup>8,9</sup> In particular, oxidation of FF to produce furoic acid (FA) (Fig. 1) is of great interest due to the application of the latter as a starting material in the agrochemical, pharmaceutical, flavour, and fragrances industries.<sup>7,10</sup>

FA is industrially produced from FF *via* a Cannizzaro reaction in the presence of a NaOH aqueous solution and strong oxidant agents, followed by an acidification step using H<sub>2</sub>SO<sub>4</sub>.<sup>11</sup> However, in the envisaged “green” context, the corrosive and toxic nature of the employed reagents makes this process undesirable.<sup>7,12</sup> Thereby, research efforts in the last

decades have aimed at accomplishing such an oxidation process in a sustainable way, avoiding the use of a base and employing “green” oxidants such as  $\text{H}_2\text{O}_2$ ,  $\text{O}_2$ , or air.<sup>13–15</sup>

Heterogeneous catalysts consisting of gold nanoparticles (AuNPs) dispersed on inorganic oxides have shown very promising results for the partial oxidation of FF under green oxidation conditions<sup>4,16-18</sup> (Table S1†). These materials' activity, selectivity, and stability are governed by different parameters such as the metal particle size, their acid-base properties, and metal-support interaction.<sup>19,20</sup> Thus, careful control of the catalyst structure constitutes a key aspect for obtaining stable catalysts while boosting the catalytic performance. Usually, higher oxidation activity is achieved only in the presence of an additional base, in aqueous or organic media. A proposed alternative to facilitate the workup procedure for product purification (neutralization of the additional homogeneous base by an acid, conventionally H<sub>2</sub>SO<sub>4</sub> as aforementioned) is to bring the necessary basicity through the use of a basic support such as MgO, CaO, or hydrotalcite, which thus involves the design of new catalysts (Table S1†). Still, catalyst stability in aqueous media can be compromised due to the leaching of the support.<sup>21,22</sup> Another drawback when working in homogeneous base-free conditions is the deactivation of the catalysts by irreversible adsorption of the formed acid on the metal surface.<sup>23,24</sup> Taking this into account, we hypothesised that encapsulating Au nanoparticles within an oxide shell could solve the issue of catalyst deactivation due to FA adsorption. Since this strategy could hinder the access of the reactants to the active site, controlling the thickness of the oxide layer

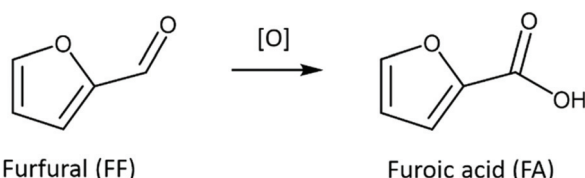


Fig. 1 Principle of synthesis of furoic acid (FA) from furfural (FF).

becomes essential. We selected  $\text{TiO}_2$  as the encapsulating oxide phase. Its non-basic character<sup>25</sup> could avoid the support leaching during the reaction, whereas its combination with Au nanoparticles have shown promising results in oxidation reactions.<sup>26</sup> This type of solids in which an oxide layer coats the metal particles has been proposed as a potential catalytic material due to enhanced control of interfacial sites which participate in the catalytic processes.<sup>27</sup> However, their catalytic applications have been scarcely studied<sup>28,29</sup> and to the best of our knowledge, they were never tested in the catalytic valorisation of biomass-derived products.

Herein, we report a highly active, selective, and stable “core–shell” material for base-free oxidation of furfural in water using air as an oxidant. The catalyst consists of  $\text{SiO}_2$ -loaded AuNPs covered by an ultra-thin  $\text{TiO}_2$  oxide shell. We found that using a fully controlled synthesis of core–shell  $\text{SiO}_2@\text{Au}@\text{TiO}_2$  materials (Fig. 2c), remarkable efficient heterogeneous catalysts can be prepared. The performance of the core–shell material was compared with a “conventional” system with AuNPs grown at the surface of a pre-formed  $\text{SiO}_2@\text{TiO}_2$  core–shell support material ( $\text{SiO}_2@\text{TiO}_2@\text{Au}$ , Fig. 2a and Fig. S3–S7†) and that of a system with AuNPs partially embedded in the  $\text{SiO}_2@\text{TiO}_2$  core–shell ( $\text{SiO}_2@\text{Au}_{\text{em}}@\text{TiO}_2$ , Fig. 2b), meaning different types of metal–oxide interactions. The result is an enhancement of the catalytic performances in the oxidation of FF when a strong metal–support interaction (SMSI) is achieved, pointing out a clear correlation between the catalyst architecture and the catalyst performance.

The studied catalysts with a 2 wt% Au nominal content were prepared by a soft chemistry method previously described by a part of the present authors.<sup>30,31</sup> To synthesize the “conventional”  $\text{SiO}_2@\text{TiO}_2@\text{Au}$  catalyst, AuNPs were loaded on pre-formed  $\text{SiO}_2@\text{TiO}_2$  core–shell nanoparticles. Well-dispersed AuNPs deposited on the  $\text{TiO}_2$  shell were obtained, as revealed by TEM analysis (Fig. 2a and Fig. S3–S7†). Then, two different solids in which the extent of the metal–support interaction was increased were prepared by a modified synthesis method, using  $\text{SiO}_2$ -loaded AuNPs as a starting material. In the  $\text{SiO}_2@\text{Au}_{\text{em}}@\text{TiO}_2$  catalyst, titanium isopropoxide (TTIP) was deposited on the surface of the  $\text{SiO}_2@\text{Au}$  catalyst without

specific control of the hydrolysis conditions (namely of pH and time). In this case, a “buried-like” structure consisting of partially embedded AuNPs was obtained.

The  $\text{TiO}_2$  shell was homogeneously deposited on the  $\text{SiO}_2$  surface *via* the intermediate titanium hydroxide ( $\text{Ti(OH)}_4$ ) formation, and Au nanoparticles were partially embedded into  $\text{TiO}_2$  (Fig. 2b). The same procedure was carried out to prepare the  $\text{SiO}_2@\text{Au}@\text{TiO}_2$  catalyst, except that we used a slow, fully controlled TTIP hydrolysis.<sup>30,31</sup> This method led to the formation of core–shell particles in which a homogeneous  $\text{TiO}_2$  shell with an average thickness of 3 nm encapsulated the AuNPs (Fig. 2c). Mean Au nanoparticle size calculated from TEM micrographs was *ca.* 5 nm in each catalyst.

The conversion achieved in the base-free oxidation of FF in water using air as an oxidant with the three Au catalysts under similar conditions is presented in Fig. 3. In addition, the blank experiment with the  $\text{SiO}_2@\text{TiO}_2$  catalyst support is shown for comparison.

The  $\text{SiO}_2@\text{TiO}_2$  catalyst support presents itself 15% conversion and yields mainly condensation products, confirming that Au is indispensable for the oxidation reaction. However, the sole presence of well-dispersed Au nanoparticles is not sufficient to boost the catalytic performance, according to the low conversion (21%) and selectivity (18%) values observed for the  $\text{SiO}_2@\text{TiO}_2@\text{Au}$  supported catalyst. The significant enhancement of the catalytic activity observed for the  $\text{SiO}_2@\text{Au}_{\text{em}}@\text{TiO}_2$  catalyst, where the  $\text{TiO}_2$  support partially embeds AuNPs, already suggests an essential role of the Au– $\text{TiO}_2$  interface. The performance shown by the  $\text{SiO}_2@\text{Au}@\text{TiO}_2$  core–shell catalyst, which quantitatively converted furfural into furoic acid, corroborates this hypothesis. The material with  $\text{TiO}_2$ -encapsulated AuNPs thus presented remarkable catalytic activity compared to its supported and embedded counterparts, with even no by-products originating from side reactions detected during the catalytic cycle. In light of the promising results with 100% carbon balance, we also studied the influence of the Au loading on the catalytic behaviour of the  $\text{SiO}_2@\text{Au}@\text{TiO}_2$  core–shell catalyst. The results are given in Table 1. Unlike the supported catalysts (Table 2), results using the core–shell materials demonstrate that the total and selec-

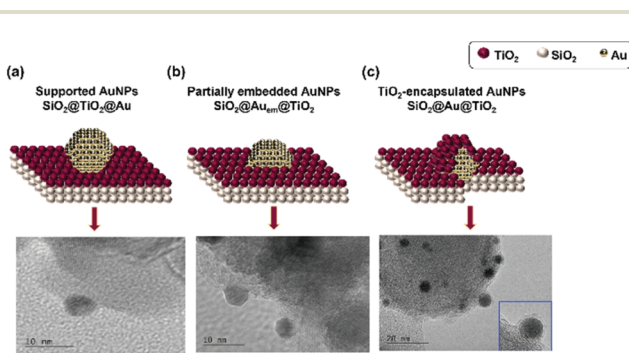


Fig. 2 Schematic representation and TEM micrographs of the prepared catalysts. (a)  $\text{SiO}_2@\text{TiO}_2@\text{Au}$ , (b)  $\text{SiO}_2@\text{Au}_{\text{em}}@\text{TiO}_2$ , (c)  $\text{SiO}_2@\text{Au}@\text{TiO}_2$ .

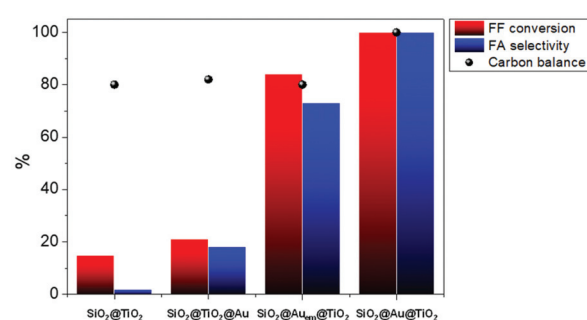


Fig. 3 FF conversion, selectivity to FA, and carbon balance over  $\text{SiO}_2@\text{TiO}_2$ , supported  $\text{SiO}_2@\text{TiO}_2@\text{Au}$ , partially embedded  $\text{SiO}_2@\text{Au}_{\text{em}}@\text{TiO}_2$  and core–shell  $\text{SiO}_2@\text{Au}@\text{TiO}_2$  catalysts (FF : Au ratio = 100, 2 h, 24 bar of air, 600 rpm).



**Table 1** FF conversion, FA selectivity, and carbon balance in the oxidation of FF over  $\text{SiO}_2@\text{Au}@\text{TiO}_2$  core–shell catalysts with different Au loadings

Catalyst	Au content (wt%)	FF conversion (%)	FA selectivity (%)	Carbon balance (%)
$\text{SiO}_2@\text{TiO}_2$	0	15	2	80
0.25% $\text{SiO}_2@\text{Au}@\text{TiO}_2$	0.13	100	>99	>99
0.5% $\text{SiO}_2@\text{Au}@\text{TiO}_2$	0.53	100	>99	>99
1% $\text{SiO}_2@\text{Au}@\text{TiO}_2$	1.13	100	>99	>99
2% $\text{SiO}_2@\text{Au}@\text{TiO}_2$	2.02	100	>99	>99

**Table 2** FF conversion, FA selectivity and carbon balance in the oxidation of FF over  $\text{SiO}_2@\text{TiO}_2@\text{Au}$  supported catalysts with different Au loadings

Catalyst	Au content (wt%)	FF conversion (%)	FA selectivity (%)	Carbon balance (%)
$\text{SiO}_2@\text{TiO}_2$	0	15	2	80
0.25% $\text{SiO}_2@\text{TiO}_2@\text{Au}$	0.28	70	12	38
0.5% $\text{SiO}_2@\text{TiO}_2@\text{Au}$	0.56	53	79	88
1% $\text{SiO}_2@\text{TiO}_2@\text{Au}$	1.26	34	56	85
2% $\text{SiO}_2@\text{TiO}_2@\text{Au}$	1.37	21	18	82

tive conversion of FF to FA can be achieved even at Au loadings as low as 0.25 wt%.

This finding could indicate that the new active species formed on the Au– $\text{TiO}_2$  interface are much more active than gold itself in the oxidation of aldehydes. However, standard characterization by XRD (Fig. S8†) and XPS (Fig. S1 and S2†) did not permit to observe differences in the  $\text{TiO}_2$  structure. Indeed, the  $\text{TiO}_2$  layer deposited on gold is very thin (1–2 nm) and XPS analysis depth is estimated of about 8 nm.

Various interpretation concerning the way Au-based catalysts activity are documented, and commented below in the light of our new results presented herein:

(i) It has been proposed for Au-supported catalysts that the accessible contact zone between the nanoparticles and the support at the bottom edge of the nanoparticles plays an important role in the catalytic performance, with the active sites located at this specific rim position at the junction between the metallic nanoparticles and the oxidic carrier.<sup>27</sup> Through this concept, optimizing the quantity of “rim sites” or “rim-like sites” could be a mean of accessing better catalytic performance.

(ii) The observed differences in the catalytic behaviour when AuNPs are supported or encapsulated under a  $\text{TiO}_2$  shell point towards a possible change in the reaction mechanism. With AuNPs exposed on the catalyst surface and in the absence of a base, the furfural molecule should adsorb on the surface-exposed gold and then follow the oxidation to the acid. Recently, Megías-Sayago *et al.*<sup>32</sup> studied the base-free oxidation of glucose to gluconic acid over Au/C catalysts and suggested that the oxidation reaction occurs preferably on gold and not on the metal–support interface or the support, in good agree-

ment with previous studies.<sup>33</sup> In this hypothesis, the reaction occurs through the formation of a carbonyl conjugated radical, which is subsequently oxidized. Since  $\text{O}_2$  dissociation is not favoured on the Au surface, the activation of  $\text{O}_2$  takes place *via* the formation and dissociation of peroxide ( $\text{OOH}^*$ ) and hydrogen peroxide ( $\text{HOOH}^*$ ) intermediates.<sup>34</sup> Consequently, in our  $\text{SiO}_2@\text{TiO}_2@\text{Au}$  supported catalysts, furfural would adsorb on AuNPs to be subsequently oxidized through hydrogen peroxide formation. Since the reaction, in this case, occurs on the Au surface, the deactivation of the catalyst is probably taking place due to the irreversible adsorption of the FA formed during the reaction.

(iii) When a  $\text{TiO}_2$  layer encapsulates AuNPs, furfural adsorption on the surface of gold should be excluded, which suggests that the oxidation process occurs through a different reaction mechanism. Whereas the  $\text{SiO}_2@\text{TiO}_2$  catalyst support favoured the formation of condensation products, our  $\text{SiO}_2@\text{Au}@\text{TiO}_2$  core–shell catalysts showed excellent catalytic performance, which confirms that the presence of Au is essential. The controlled architecture of the  $\text{SiO}_2@\text{Au}@\text{TiO}_2$  catalyst generates an enhanced gold–titania surface interaction, with the active sites presumably located in the periphery of the  $\text{TiO}_2/\text{Au}$  interface. In fact, some research groups have recently proposed the Au-assisted Mars–van Krevelen mechanism as possibly occurring during CO oxidation over Au/ $\text{TiO}_2$  catalysts, which entails the participation of lattice oxygen atoms near the periphery of Au/ $\text{TiO}_2$  in the oxidation process. The desorption of  $\text{CO}_2$  formed generates an oxygen vacancy, which is subsequently replenished by  $\text{O}_2$ .<sup>35–37</sup> The presence of Au in close interaction with the  $\text{TiO}_2$  support plays a fundamental role, presumably facilitating the formation of oxygen lattice vacancies in the Au/ $\text{TiO}_2$  perimeter thanks to the ability of gold to accommodate the excess electrons generated during the oxygen vacancies formation. Thus, in our case, furfural could adsorb on  $\text{TiO}_2$  and react with the lattice oxygen atoms located at the periphery of the  $\text{TiO}_2/\text{Au}$  interface. The oxidation of furfural to furoic acid could proceed through the Au-assisted Mars–van Krevelen mechanism, that is, *via* the cyclic formation and replenishment of oxygen vacancies. Another possible mechanism could imply the adsorption of furfural on the surface of  $\text{TiO}_2$  and its subsequent oxidation through the formation of hydrogen peroxide on gold. Such a mechanism could take place assuming that diffusion of  $\text{O}_2$  through the  $\text{TiO}_2$  layer is possible. Regardless of the reaction path, furfural adsorption does not occur on the surface of the metal particles, which prevents the accumulation of reaction products on the metal surface leading to catalyst deactivation.

According to these hypotheses, the catalytic behaviour of the  $\text{SiO}_2@\text{Au}_{\text{em}}@\text{TiO}_2$  catalyst could be explained by the simultaneous occurrence of both mechanisms since Au can be found both on the surface or partially embedded in the  $\text{TiO}_2$  layer.

The present results pave the way towards the design of highly efficient catalysts for oxidation reactions. We demonstrate using variable catalyst design that the  $\text{TiO}_2/\text{Au}$  interface has a key role in the reported enhancement of FF oxidation. Nevertheless, how the furfural oxidation proceeds in such a



complex catalytic system is an aspect needing to be clarified. Thus, DFT studies and deep characterization of these materials are in progress to elucidate the mechanism of this reaction and the real nature of the extremely efficient active site.

## Conclusions

TiO<sub>2</sub>-encapsulated AuNPs, SiO<sub>2</sub>@Au@TiO<sub>2</sub> core–shell catalysts, have proved excellent activity, selectivity, and stability in the base-free oxidation of furfural using air as an oxidant. The materials showed a hundredfold catalytic activity increase with respect to conventional supported Au catalysts (SiO<sub>2</sub>@TiO<sub>2</sub>@Au), even using very low gold loadings, with 100% selectivity. The activity enhancement process could be explained by a change in the reaction mechanism induced by an extended TiO<sub>2</sub>–Au interaction in the core–shell catalysts. In the supported catalysts, furfural adsorption would take place on AuNPs, and possibly the deactivation of the catalyst is due to furoic acid adsorption. In the case of the core–shell catalysts, furfural adsorption would take place on the very thin TiO<sub>2</sub> layer just covering the metal particles, thus avoiding the irreversible adsorption of the acid on gold and the subsequent catalyst deactivation. Our results demonstrate how the increase in the extent of the interface between the support and metal significantly increases the overall catalytic activity *via* a synergic effect between both components. Indeed, once embedded, the stability of gold increases and the adsorption of the reaction products on the surface of gold is excluded. Consequently, this work provides new insights into the design of heterogeneous catalysts, suggesting that the core–shell SiO<sub>2</sub>@Au@TiO<sub>2</sub> catalysts could be used for various oxidation processes, even under harsh conditions.

## Author contributions

CPF: Conceptualization, data curation, formal analysis, writing – original draft, SNJ: data curation, writing – original draft, LMR: funding acquisition, supervision, validation, writing – review & editing, FD: supervision, validation, writing – review & editing, MNG: conceptualization, formal analysis, methodology, validation, writing – review & editing, RW: conceptualization, project administration, supervision, writing – original draft, writing – review & editing.

## Conflicts of interest

The authors declare no conflict of interest.

## Acknowledgements

LMR is grateful to FAPESP (2016/16738-7, 2018/26253-6) for financial support. LMR acknowledges CNPq (306024/2019-5).

The financial support of this work was provided by the French National Research Agency (ANR), through the IngenCat project (ANR-20-CE43-0014).

## Notes and references

- 1 R. Calvo-Serrano, M. Guo, C. Pozo, Á. Galán-Martín and G. Guillén-Gosálbez, *ACS Sustainable Chem. Eng.*, 2019, **7**, 10570–10582.
- 2 S. A. Montzka, E. J. Dlugokencky and J. H. Butler, *Nature*, 2011, **476**, 43–50.
- 3 C. M. Liu, N. K. Sandhu, S. T. McCoy and J. A. Bergerson, *Sustain. Energy Fuels*, 2020, **4**, 3129–3142.
- 4 R. Wojcieszak, C. P. Ferraz, J. Sha, S. Houda, L. M. Rossi and S. Paul, *Catalysts*, 2017, **7**, 352.
- 5 J. N. Chheda, G. W. Huber and J. A. Dumesic, *Angew. Chem., Int. Ed.*, 2007, **46**, 7164–7183.
- 6 A. Corma, S. Iborra and A. Velty, *Chem. Rev.*, 2007, **107**, 2411–2502.
- 7 P. L. Arias, J. A. Cecilia, I. Gandarias, J. Iglesias, M. López Granados, R. Mariscal, G. Morales, R. Moreno-Tost and P. Maireles-Torres, *Catal. Sci. Technol.*, 2020, **10**, 2721–2757.
- 8 D. Y. Murzin, E. Bertrand, P. Tolvanen, S. Devyatkov, J. Rahkila, K. Eränen, J. Wärnå and T. Salmi, *Ind. Eng. Chem. Res.*, 2020, **59**, 13516–13527.
- 9 J. J. Bozell and G. R. Petersen, *Green Chem.*, 2010, **12**, 539.
- 10 A. E. Eseyin and P. H. Steele, *Int. J. Adv. Chem.*, 2015, **3**, 42.
- 11 K. J. Zeitsch, in *The chemistry and technology of furfural and its many by-products*, Elsevier B. V., Amsterdam, 2000, vol. 13, ch. 19, pp. 159–163.
- 12 C. Xu, E. Paone, D. Rodriguez-Padron, R. Luque and F. Mauriello, *Chem. Soc. Rev.*, 2020, **49**, 4273–4306.
- 13 C. P. Ferraz, N. J. S. Costa, E. Teixeira-Neto, Â. A. Teixeira-Neto, C. W. Liria, J. Thuriot-Roukos, M. T. Machini, R. Froidevaux, F. Dumeignil, L. M. Rossi and R. Wojcieszak, *Catalysts*, 2020, **10**, 75.
- 14 F. Menegazzo, T. Fantinel, M. Signoretto, F. Pinna and M. Manzoli, *J. Catal.*, 2014, **319**, 61–70.
- 15 C. Megías-Sayago, S. Navarro-Jaén, R. Castillo and S. Ivanova, *Curr. Opin. Green Sustain. Chem.*, 2020, **21**, 50–55.
- 16 E. Taarning, I. S. Nielsen, K. Egeblad, R. Madsen and C. H. Christensen, *ChemSusChem*, 2008, **1**, 75–78.
- 17 F. Menegazzo, M. Manzoli, A. di Michele, E. Ghedini and M. Signoretto, *Top. Catal.*, 2018, **61**, 1877–1887.
- 18 M. Douthwaite, X. Huang, S. Iqbal, P. J. Miedziak, G. L. Brett, S. A. Kondrat, J. K. Edwards, M. Sankar, D. W. Knight, D. Bethell and G. J. Hutchings, *Catal. Sci. Technol.*, 2017, **7**, 5284–5293.
- 19 C. Ampelli, K. Barbera, G. Centi, C. Genovese, G. Papanikolaou, S. Perathoner, K. J. Schouten and J. K. van der Waal, *Catal. Today*, 2016, **278**, 56–65.
- 20 N. Dimitratos, C. Hammond and P. P. Wells, in *Gold Catalysis: Preparation, Characterization, and Applications*, ed. L. Prati and A. Villa, CRC Press, Boca Raton, 2015.



21 C. P. Ferraz, M. Zieliński, M. Pietrowski, S. Heyte, F. Dumeignil, L. M. Rossi and R. Wojcieszak, *ACS Sustainable Chem. Eng.*, 2018, **6**, 16332–16340.

22 A. Roselli, Y. Carvalho, F. Dumeignil, F. Cavani, S. Paul and R. Wojcieszak, *Catalysts*, 2020, **10**, 73.

23 M. Besson and P. Gallezot, *Catal. Today*, 2000, **57**, 127–141.

24 S. Chen, R. Wojcieszak, F. Dumeignil, E. Marceau and S. Royer, *Chem. Rev.*, 2018, **118**, 11023–11117.

25 E. Farfan-Arribas and R. J. Madix, *J. Phys. Chem. B*, 2003, **107**, 3225–3233.

26 Z. Duan and G. Henkelman, *ACS Catal.*, 2015, **5**, 1589–1595.

27 J. Zhang and J. Will Medlin, *Surf. Sci. Rep.*, 2018, **73**, 117–152.

28 C. Wu, L. Lin, J. Liu, J. Zhang, F. Zhang, T. Zhou, N. Rui, S. Yao, Y. Deng, F. Yang, W. Xu, J. Luo, Y. Zhao, B. Yan, X. D. Wen, J. A. Rodriguez and D. Ma, *Nat. Commun.*, 2020, **11**, 5767.

29 G. Wang, F. Luo and F. Zhao, *React. Kinet., Mech. Catal.*, 2021, **132**, 155–170.

30 G. D. Gesesse, C. Wang, B. K. Chang, S. H. Tai, P. Beaunier, R. Wojcieszak, H. Remita, C. Colbeau-Justin and M. N. Ghazzal, *Nanoscale*, 2020, **12**, 7011–7023.

31 G. D. Gesesse, T. Le Neel, Z. Cui, G. Bachelier, H. Remita, C. Colbeau-Justin and M. N. Ghazzal, *Nanoscale*, 2018, **10**, 20140–20146.

32 C. Megías-Sayago, L. F. Bobadilla, S. Ivanova, A. Penkova, M. A. Centeno and J. A. Odriozola, *Catal. Today*, 2018, **301**, 72–77.

33 T. Ishida, N. Kinoshita, H. Okatsu, T. Akita, T. Takei and M. Haruta, *Angew. Chem., Int. Ed.*, 2008, **47**, 9265–9268.

34 B. N. Zope, D. D. Hibbitts, M. Neurock and R. J. Davis, *Science*, 2010, **330**, 74–78.

35 P. Mars and D. W. van Krevelen, *Chem. Eng. Sci.*, 1954, **3**, 41–59.

36 M. A. Saqlain, A. Hussain, M. Siddiq and A. A. Leitão, *Appl. Catal., A*, 2016, **519**, 27–33.

37 P. Schlexer, D. Widmann, R. J. Behm and G. Pacchioni, *ACS Catal.*, 2018, **8**, 6513–6525.

